ELSEVIER
SAUNDERS

Dent Clin N Am 52 (2008) 731–752

THE DENTAL
CLINICS
OF NORTH AMERICA

Cone Beam Tomographic Imaging Anatomy of the Maxillofacial Region

Christos Angelopoulos, DDS, MS

Division of Oral and Maxillofacial Radiology, Columbia University, College of Dental Medicine, PH-7 Stem-134, New York, NY 10032, USA

The main challenge in cone beam CT (CBCT) imaging and diagnosis is the lack of familiarity experienced by most dental professionals with the concept of multiplanar imaging that is offered by this new and exciting technology. Dentists and specialists, with only a few exceptions, have a wide experience in diagnosis using the traditional dental imaging modalities (intraoral radiography and panoramic radiography), and the comfort level in their diagnostic skills with these modalities is high. These imaging modalities have been taught for several decades in the dental schools and in other training courses.

Diagnostic imaging in different planes is a new concept and may require a different view of the imaging data. It is reminded that multiplanar imaging or reformatting is the ability to generate images in different planes, flat or curved. This ability is offered only by some contemporary imaging modalities, such as CBCT, medical CT, MRI, ultrasound, and others. Because a volume of data has been acquired and stored by CBCT, these data can be reformatted or realigned and several different types of images can be synthesized in any way the diagnostician requires. With multiplanar imaging, the diagnostician or operator can recreate images in different planes (flat or curved) with simple functions. This increases the diagnostic efficiency in the hands of the knowledgeable individual in an unparalleled way (Fig. 1).

In this article, the author reviews the appearance of several anatomic structures of the maxillofacial region and the head and neck region in general; these structures are revealed in a variety of planes (eg, axial, coronal, sagittal, and more). What may add to the complexity of these images is the fact that this technology may demonstrate structures of interest, such as teeth and jaws, in a view that dental professionals have not seen in the past; dentists were never able to view the third dimension of the regions

E-mail address: ca2291@columbia.edu

doi:10.1016/j.cden.2008.07.002 *dental.theclinics.com*

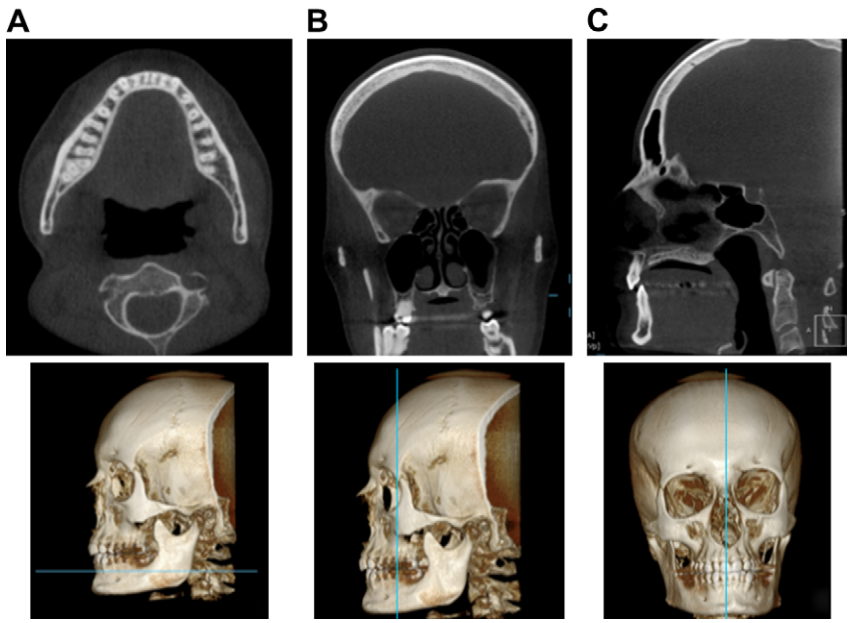

Fig. 1. Multiplanar imaging and reformatting. Axial (*A*), coronal (*B*), and sagittal (*C*) sections of the head. The approximate tomographic plane is shown in the three-dimensional images (*blue line*). These sections can be generated with simple functions using the CBCT scanner's software applications.

of interest. From the beginning, this may make the images look unfamiliar and different.

First, as with every other dental diagnostic image, the images are viewed as if the patient under examination were sitting opposite the dentist, as in the dental chair. The structures identified on the dentist's right side would represent the anatomic structures on the patient's left and vice versa. Most of the available software of the various manufacturers properly identifies the right and left sides or the buccal and lingual sides of the images; thus, orientation is not difficult.

The author starts with the evaluation of well-known dental structures in the maxillofacial region in cross sections. Cross-sectional images are generated perpendicular to the arch-form of the maxilla or mandible. The image demonstrated in Fig. 2 is a cross-sectional image (cut or slice) of the maxilla and mandible in the first molar location. In this image, the buccal and palatal or lingual sides are clearly identified.

The maxillary sinus is a pyramidal in shape low-density (black or dark) structure. The appearance of healthy air cavities in the maxillary sinuses is dark (black) because of the fact that air attenuates x-rays minimally. The thin cortical outline of the buccal and medial sinus walls can be identified in these images. The medial wall of the maxillary sinus borders the sinus

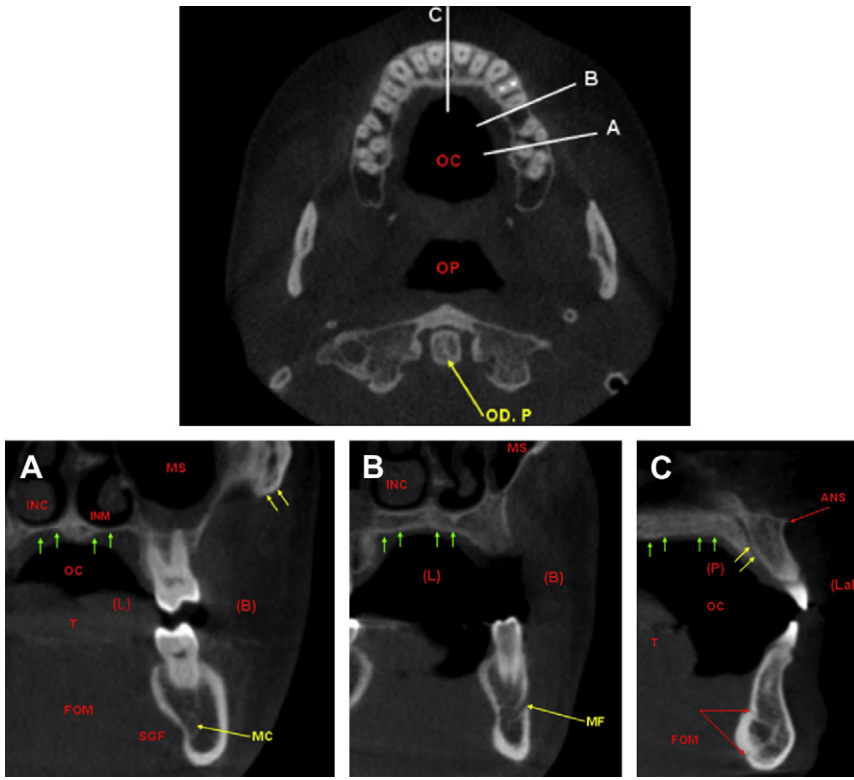

Fig. 2. Axial image (*upper*) at the level of the maxillary alveolar ridge demonstrates the approximate locations of the cross sections A, B, and C. The white lines correspond to the respective sections: odontoid process of axis (ODP) and second cervical vertebra. (*A*) Cross-sectional images in the molar region: the buccal (B), labial (Lab), lingual (L), or palatal (P) aspect of the alveolar bone is marked on the images. FOM, floor of mouth; INC, inferior nasal concha; INF, inferior nasal meatus; MC, mandibular canal; MS, maxillary sinus; OC, oral cavity; SGF, submandibular gland fossa; T, tongue. The green arrows indicate the hard palate, and the yellow arrows indicate the zygomatic process of the maxilla. Note the presence of inflammatory tissue on the floor of the maxillary sinus. The air cavities appear dark (*black*) in CT images. (*B*) Premolar region: MS, maxillary sinus; INC, inferior nasal concha; INF, inferior nasal meatus; OC, oral cavity; T, tongue; FOM, floor of mouth; MF, mental foramen. The green arrows indicate the hard palate. (*C*) Central incisor region: the buccal (B), (Lab), (L), or (P) aspect of the alveolar bone is marked on the images. ANS, anterior nasal spine; OC, oral cavity; T, tongue. The green arrows mark the hard palate, the yellow arrows show the nasopalatine canal, and the red arrows show the lingual foramina (superior and inferior).

cavity from the nasal cavity. Note the soft tissue coverage of the nasal cavity being demonstrated as gray in the image. The high-density core is the inferior nasal concha. The reader is reminded that the inferior nasal concha is an independent facial bone, whereas the rest of the conchae, middle and superior nasal conchae, are parts of the ethmoid bone. Also note that the soft tissue in the region (intraoral and extraoral) demonstrates an almost

uniform density; CBCT soft tissue contrast is not adequate to demonstrate differences in musculature or fat, for example.

Further inferior in the same image, you can identify a cross section of the mandibular molar region and the long axis of the mandibular bone in the cross section. Note that the mandibular teeth are not always parallel with the long axis of the mandibular bone in the cross section. The cortical outline of the mandibular bone appears to be much thicker than that of the maxilla (discussed previously). Moreover, the submandibular gland fossa sometimes is more prominent than others. This undercut can be rather severe at times and may impose an anatomic limitation in implant placement in the region. Last, significant anatomic structures, such as the lingual artery, are passing nearby. The mandibular canal is identified into the mandibular bone.

As we move more anteriorly, we are examining cross-sectional images in the premolar locations. You can see similar anatomic structures as the ones before; however, the further anterior we go, the narrower the maxillary sinuses become because we are approaching the anterior wall of the maxillary sinuses. In this cross section, we can see the anterior opening of the mandibular canal, which is the mental foramen. There is considerable variation in the appearance of the mental foramen and its emergence angle (opening angle) into the buccal aspect of the mandibular bone.

The next cross section is along the midline of the maxilla and the mandible, and some different anatomic structures are seen: in this case, the floor of the nasal cavity and the nasopalatine canal. The reader is reminded that the nasopalatine canal starts from the floor of the nasal cavity (inferior meatus) with dual foramina (superior foramina). It carries branches of the nasopalatine nerve, which exit the canal through the incisive foramen and spread to the anterior aspect of the hard palate (see Fig. 2C). The nasopalatine canal may vary in dimensions, and also may pose a limitation in placing implants in this aesthetic zone, the anterior maxilla.

Once more, great variation exists concerning the shape of the anterior mandible in cross sections. A significant anatomic structure in the lingual aspect of the mandibular bone, along the midline of the mandible, is the lingual foramen or foramina, which accommodate the terminal branches of the lingual artery (see Fig. 2C; Fig. 3). Often, they are closely associated with the genial tubercles (high-density structures), which serve as muscle attachment points. The diameter of these canals or foramina is related to the blood-supplying capacity of the blood vessel, and as a result, if they are wide enough, they may bleed significantly if injured during surgical procedures, such as implant surgery [1]. Despite the fact that they are located toward the inferior third of the mandibular bone, they may be seen closer to the crest pending atrophy of the anterior alveolar ridge.

Additional vascular canals are noted from time to time in the mandibular bone anterior to the premolar locations in a region that generally is considered to be a safe site for implant placement (interforaminal region). These

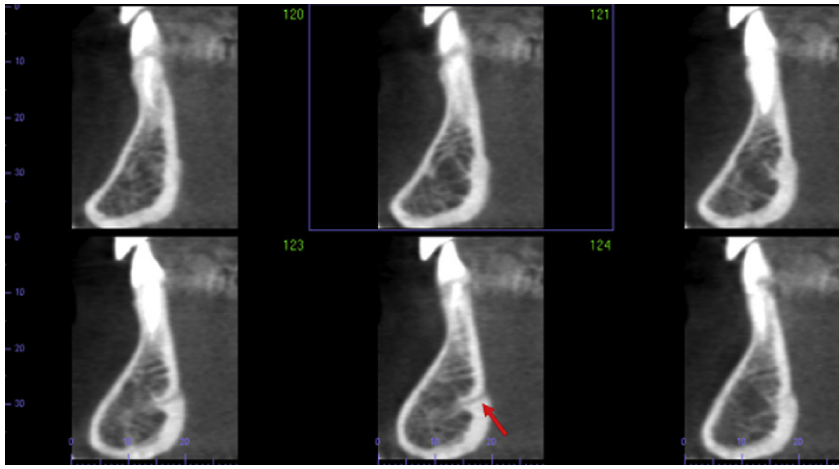

Fig. 3. A series of cross-sectional images in the mandibular central incisor region. The narrow opening in the lingual mandibular cortex (*red arrow*) is the lingual foramen, a vascular canal along the midline, through which the terminal branches of the lingual artery enter the mandibular bone. This canal has been reported as a concern for significant bleeding (pending on its diameter) if punctured during implant surgery.

canals often represent accessory lingual foramina that host accessory branches of the lingual artery. Depending on the width, they may also pose limitations for surgical procedures [2]. Once more, these foramina are identified fairly inferior, unless severe bone resorption is noted (Fig. 4).

The variation of the shape and size of the alveolar ridge is remarkable. After tooth extraction, the maxillary bone and mandibular bone rarely remain unchanged. Frequently, the edentulous areas are accompanied by undercuts as a result of bone resorption, and these undercuts may pose anatomic limitations in implant placement in the posterior mandible (Figs. 5 and 6).

The reader has now become familiar with the cross-sectional imaging of the major anatomic structures in the oral cavity that the dentist frequently uses and identifies in routine dental radiographs. The author now examines these anatomic structures among others in different planes: axial, coronal, and sagittal planes. Once more, these images are reviewed as if the patient were opposite the dentist. Consequently, the right side of the patient's face or the right anatomic structures are on the dentist's left and vice versa. Axial sections (cuts) are the images that have been generated perpendicular to the long axis of the human body (the long axis of the head in this case). These images section the teeth perpendicular to their long axis; as a result, the dentist is able to see transverse sections of the roots and crowns of the teeth in the areas of interest.

Axial images are excellent for the evaluation of the visible parts of the neck and cervical spine, integrity of the palatal and buccal cortical plates

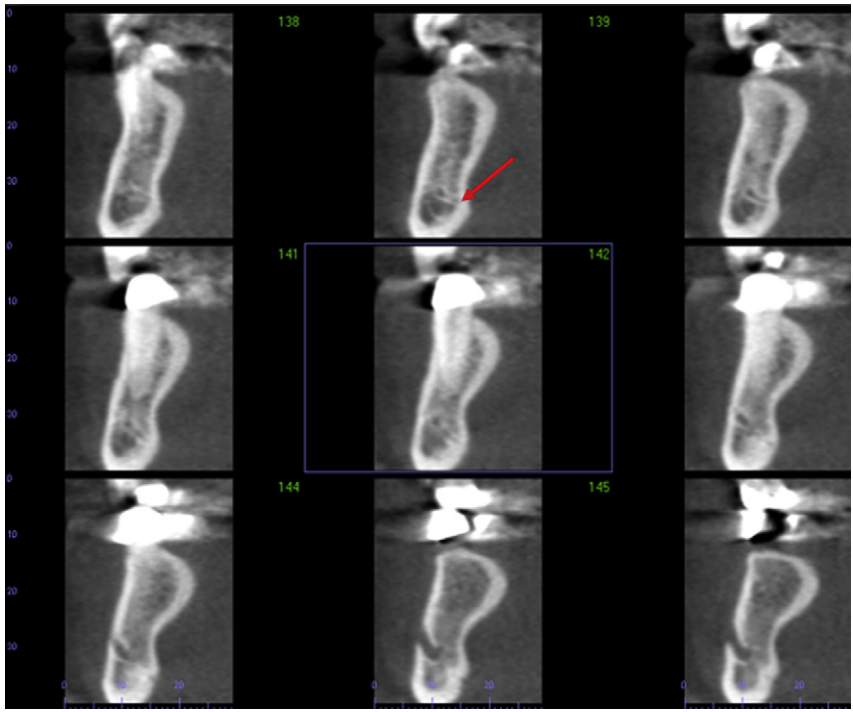

Fig. 4. Accessory lingual foramina. Although not as frequently as the lingual foramina (*red arrow*) noted along the midline of the mandible, additional vascular channels may be present anterior to the premolar locations unilaterally or bilaterally. Depending on their diameter, they may pose a similar limitation to implant surgery as their midline counterparts.

of the maxillary and mandibular dentition, lateral and medial wall of the sinuses, lateral walls of the nasal cavity, anatomic structures in the nasal cavity, zygomatic bones and zygomatic arches, and skull base, for example.

Only parts of the patient's neck can be visualized toward the inferior end of the imaging volume. Soft tissue structures are mostly present at that level (Fig. 7). The inferior border of the anterior mandible may be sectioned at this level and may be visualized toward the superior border of the image. The hyoid bone and the body and the processes of the C3 to C4 vertebrae are expected to be seen in the same cuts. The soft tissue structures identified in this image include the sternocleidomastoid muscles bilaterally, the geniohyoid muscles, and the submandibular salivary glands. In the center of the image, this semicircular low-density (dark structure) in the middle of the image represents the patient's airway. The airway is separated almost in two halves by a soft tissue structure that is crescent in shape (and some times irregular in appearance), the epiglottis. Approximately at this level, the common carotid artery bifurcates into two main branches, the internal carotid and external carotid arteries, which supply the brain and face of each

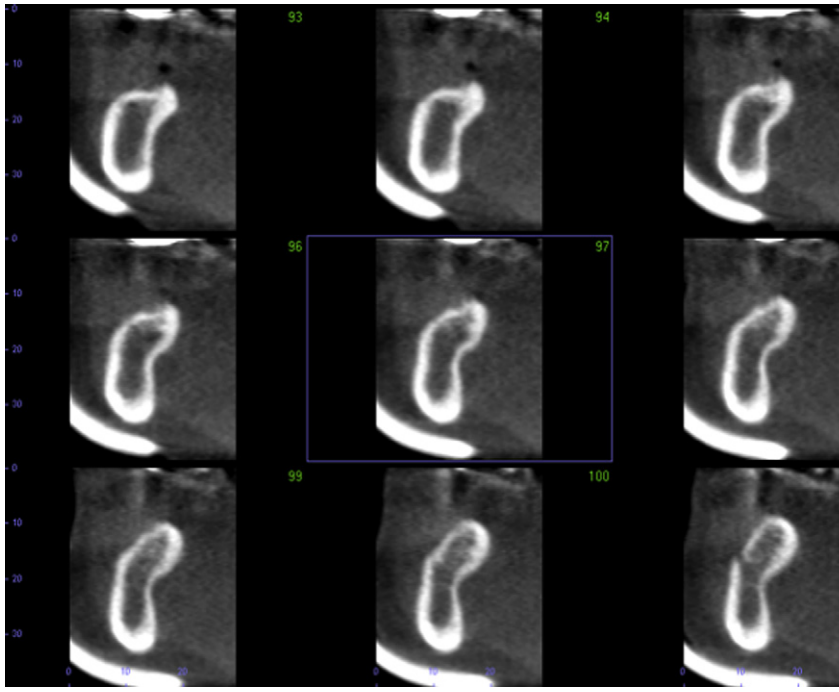

Fig. 5. Alveolar ridge variation. A series of cross-sectional cuts in the mandibular premolar and molar areas shows a marked lingual inclination of the tooth-bearing part of the alveolar bone. Moreover, a lingual undercut is noted extending to the premolar regions (*lower three cross sections*).

side, respectively. The most reliable reported landmarks to indicate the level at which bifurcation occurs are the C3 and C4 levels and the superior border of the thyroid cartilage of the larynx; however, variation is not uncommon (see Fig. 7; Fig. 8). Superior to the bifurcation, the blood vessels are less distinguishable because of their reduced diameter.

Despite the fact that the major blood vessels of the neck discussed previously are rarely distinguished from the rest of the soft tissues of the neck in CBCT images because of the limited soft tissue contrast (see Fig. 8), knowledge of and familiarity with the course of the blood vessel on the lateral neck is crucial to identify pathologic conditions inside or in the vicinity of the blood vessels, such as carotid artery atheromatosis, a pathologic condition in which calcified deposits (atheromas) accumulate on the internal wall of the blood vessel; this gradually reduces the flexibility and functionality of the blood vessel. Carotid artery atheromatosis demonstrates a fairly high incidence rate in older age groups and has been associated with an increased risk for stroke [3]. These calcifications most frequently occur within 10 to 15 mm of the bifurcation (above or below). Sometimes, they have a clear tubular appearance that makes them more readily identifiable than not. Other times, they look more like a cluster of calcifications in the region (Fig. 9).

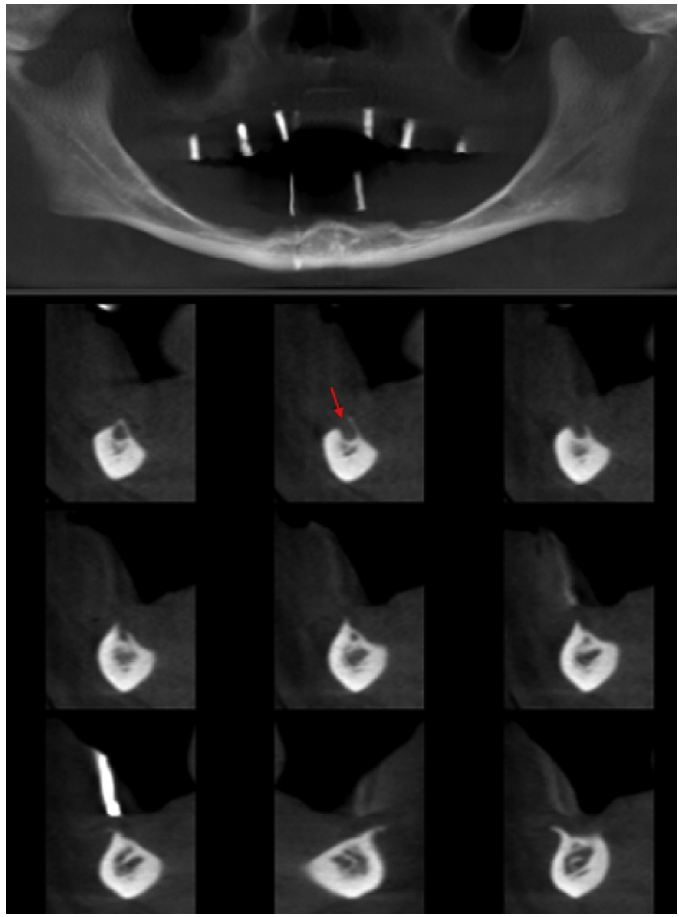

Fig. 6. Severe atrophy of the alveolar ridge. Panoramic (upper) and cross-sectional images of an edentulous patient who presented for preimplant assessment (see opaque markers on the crest of the alveolar ridge). The mandibular alveolar ridge demonstrates severe atrophy. The mental foramen now opens on the crest of the ridge (*red arrow*). Note the small well-defined lucent area just anterior to the mental foramen just inferior to the crest. This small channel hosts the continuation of the inferior alveolar nerve, which is known as the incisive branch of the inferior alveolar nerve. This continues towards the midline, past the mental foramen.

Other types of neck calcifications may include calcifications in the thyroid cartilage complex, stylohyoid ligament calcifications, sialoliths, and tonsilloliths (Figs. 10 and 11). Some may resemble carotid artery calcifications; however, the appearance and location should assist in determining the origin of the calcification most of the time.

Apart from the visualization of the corresponding cervical vertebrae (depending on the level of the axial sections) and the mandibular bone, axial images of the floor of the mouth reveal minimal information about the soft tissue structures in the region (Fig. 12).

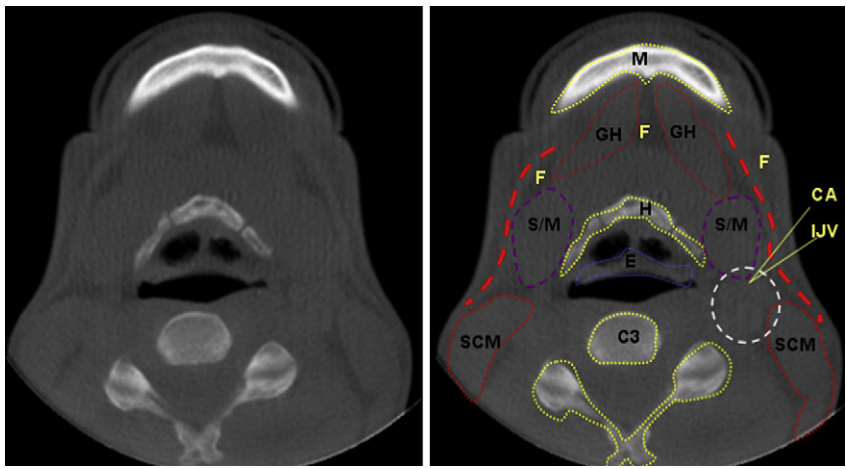

Fig. 7. (*Left*) Axial CBCT image at the level of the hyoid and C3 vertebra. (*Right*) Same axial image as the one on the left with some identifiable neck anatomic structures outlined (despite the fact that the soft tissue contrast of CBCT is not optimal for the diagnosis of soft tissue pathologic conditions, some of the neck anatomic landmarks are visualized). H, hyoid bone; M, inferior border of the anterior mandible. Note the almost modular appearance of the hyoid bone that can imitate a fracture. C3, axial section of the third cervical vertebra; E, epiglottis; F, fatty tissue; GH, geniohyoid muscle; SCM, sternocleidomastoid muscle; S/M, submandibular salivary glands. Because of the fact that they are mainly occupied by fat, the neck spaces appear of a lower density in comparison to the neighboring musculature. CA, carotid arteries, IJV, internal jugular vein. Please note that this is the approximate location of the major blood vessels of the neck; their precise location cannot be clearly seen without the use of intravenous administration of contrast media. Knowledge of the topographic location of the major neck anatomic structures can assist the diagnostician to determine the origin of the various pathologic entities that may develop on the neck.

Sagittal images of the neck are best for the assessment of the cervical spine and the airway (Fig. 13). The cervical spine is only partially visualized in a CBCT scan (C1–C4). The normal (healthy) appearance of the vertebral bodies includes a fairly square body, a thin cortical outline, a cancellous component of homogeneous density, and a fairly symmetric spacing between the vertebrae visible in the scan. Pathologic findings associated with the cervical spine and other irregularities are not uncommon. Often, these are incidental findings in scans that were prescribed for different reasons (see Fig. 13B, C).

The airway is identified as an irregularly shaped, elongated, low-density (dark) area anterior to the cervical part of the vertebral column. The position of the epiglottis, the laryngeal opening below the epiglottis, and the position of the tongue may have an effect on the diameter of the airway in several locations. CBCT images are useful in the evaluation of the airway and the factors that may cause restrictions in the airflow in sleep apnea cases (Fig. 14).

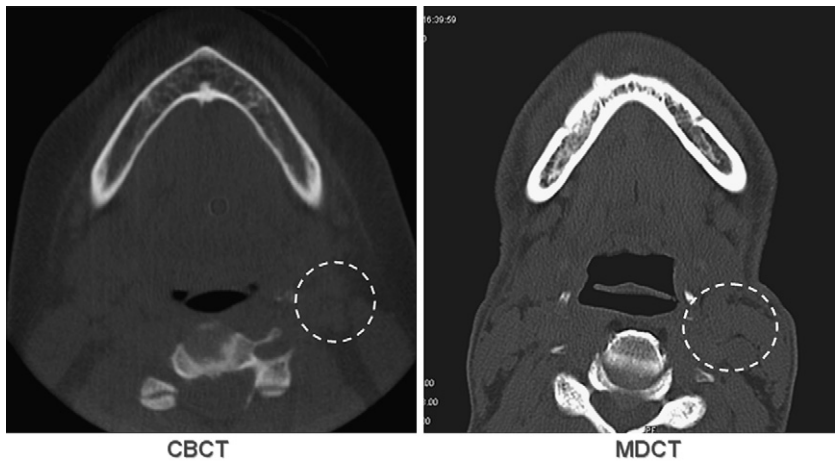

Fig. 8. Soft tissue contrast between CBCT and multidetector CT (MDCT). CBCT axial image at the level of C3 (*left*) and MDCT (*right*). Note the higher soft tissue contrast for MDCT images and the sharper depiction of structures like muscles and blood vessels, for example. The dotted ring outlines the region where the major blood vessels of the neck most frequently appear. The three round well-defined soft tissue structures seen in the marked area on the MDCT image medial to the SCM muscle may represent the carotid arteries and the internal jugular vein. On the contrary, the same region seems to be rather unclear in the CBCT axial image.

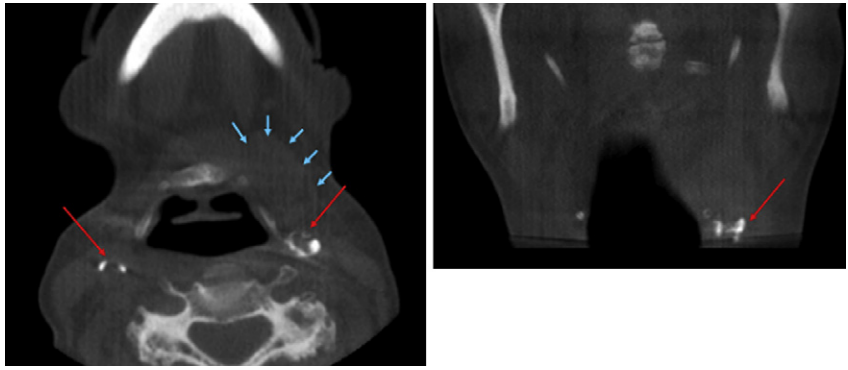

Fig. 9. Axial and coronal images of the neck. Bilateral circular calcifications are noted at the level of C3 and C4, toward the posterolateral wall of the airway, just medial to the anterior border of the SCM (*red arrows*). These are carotid artery calcifications attributable to atheromatosis. Note that the appearance of the left (L) calcification in the coronal image resembles the lumen of a vessel. Also, note the marked neck asymmetry between the right and left sides of the neck. This is attributable to prior surgical removal of the right submandibular (SM) gland. The left SM gland is outlined by the blue arrows.

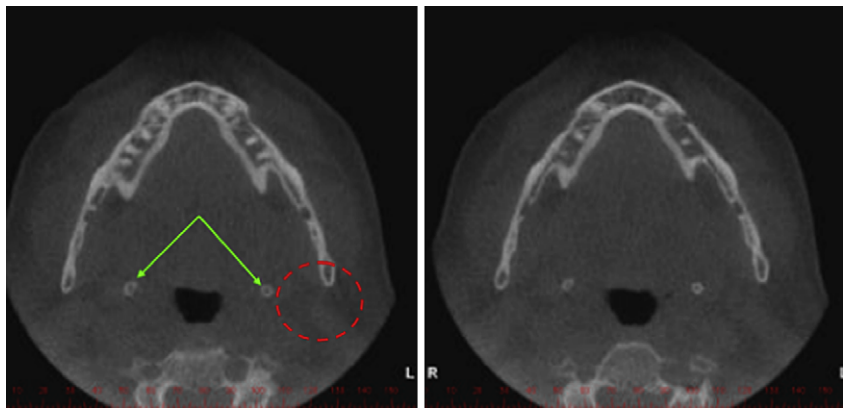

Fig. 10. Bilateral calcifications of the stylohyoid ligaments (*green arrows*). Note the close proximity to the location of the major blood vessels of the neck where carotid artery calcifications may occur (*round dotted region*). Also note the deep right and left submandibular gland depressions on the lingual aspect of the mandible (*Courtesy of* S. Thomas, DDS, MD, MS, Overland Park, KS).

The midfacial structures and the skull base are reviewed next in a series of axial sections (Figs. 15–20). Apart from the apices of the maxillary teeth, the hard palate, and the floor of the maxillary sinuses, the superior foramina (anteriorly) and the greater and lesser palatine foramina are visualized at that level. The former are the entrance of the nasopalatine canal and are located on the floor of the nasal cavity (inferior meatus), and they host the nasopalatine nerve. The latter serve as the opening to the greater and lesser palatine nerves and vessels that run the hard palate from posterior to anterior just superior to the palatal roots of the maxillary molars in the soft tissue in a palatal mucosa (see Fig. 15). Their identification during palatal

Fig. 11. Bilateral calcifications (*arrows*) at the level of the floor of the mouth (axial and coronal images). Note the superficial location of the calcifications in relation to the airway. These were tonsillar calcifications or tonsilloliths. These are frequently associated with recurrent inflammation of the tonsils.

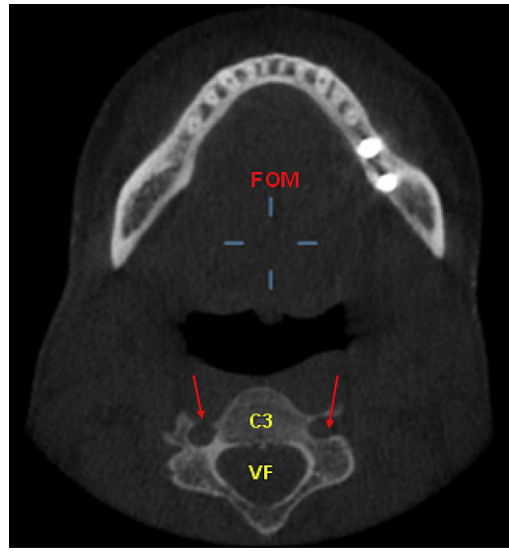

Fig. 12. Axial cut of the mandible toward the lower half of the mandibular body. At that level, the C3 vertebra is depicted. VF, vertebral foramen. The red arrows mark the right and left transverse foramen (or foramen transversarium). Contiguous transverse foramina form a canal that hosts the vertebral artery during its ascending course toward the endocranium. FOM, floor of the mouth. Note that because of inadequate soft tissue contrast, it is impossible to distinguish different soft tissue structures in the mouth.

surgery and palatal flap elevation is important. Similar to several other important anatomic structures, they cannot always be visualized in CBCT scans.

The nasopharyngeal aspect of the airway dominates the center of the axial cuts of the midface. Its shape and size varies and may be affected by neighboring anatomic structures in the vicinity. A deep depression on the lateral walls of the nasopharynx bilaterally is the Eustachian tube, the tube that communicates and balances the air pressure between the inner ear and external ear (see Fig. 15). Just posterior to the Eustachian tube, separated only by a soft tissue projection (torus tubarius), lies the pharyngeal recess or fossa of Rosenmüller. The fossa of Rosenmüller has been associated with pathologic entities. This region is almost always going to appear in the maxillary CBCT scans, and it is imperative that it be included in an evaluation. Further dorsally, an ovoid or ellipsoid structure is visualized toward the anterior aspect of the foramen magnum; this is the odontoid process of the axis (see Fig. 2, axial image).

Axial cuts made more cephalad reveal the right and left maxillary sinuses (see Fig. 16). Almost pyramidal in shape, with the base of the pyramid being the medial wall or the wall that is shared with the nasal cavity and the other two sides, are the anterior wall and the posterior wall. As mentioned

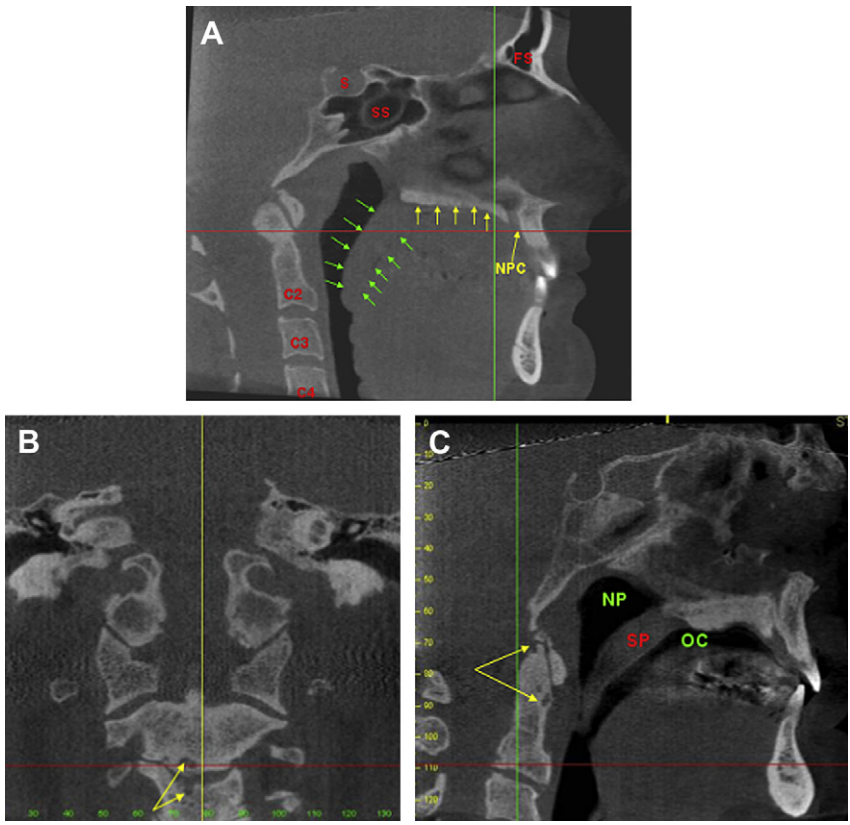

Fig. 13. (*A*) Midsagittal cut of the face and neck. Sagittal sections are best for the evaluation of the visible portion of the cervical spine and the airway. C2, second cervical vertebra-axis; C3, third cervical vertebra-axis; C4, fourth cervical vertebra-axis; FS, frontal sinus; NPC, nasopalatine canal; S, sella turcica; SS, sphenoid sinus. The yellow arrows mark the hard palate, and the green arrows mark the soft palate. The elongated, slightly curved, low-density area anterior to the cervical spine is the airway. Coronal (*B*) and sagittal (*C*) images of the same case demonstrate clear evidence of degenerative joint disease in the visible part of the cervical spine. The yellow arrows show erosive lesions or small subchondral cysts in the C2 and C3 vertebral bodies. Other signs of degenerative joint disease (arthritis) include loss of intervertebral space, osteophyte formation, and sclerosis, for example. In the sagittal image (*C*), the soft palate (SP) separates the upper airway into two distinct parts: the nasopharynx (NP) and the oral cavity (OC).

previously, all the air cavities are demonstrated as absolute black because of the fact that air is depicted as a low-density structure in CT. The presence of any other appearance other than black may represent a pathologic finding in the air cavity. As far as the nasal cavity is concerned, the structures being sectioned are elongated structures running the nasal cavity from anterior to posterior; these are the inferior nasal conchae and their soft tissue outline

Fig. 14. A thick sagittal cut visualized in three dimensions to assess the airway shown in blue. Several software programs (mostly third party) offer specific utilities that simplify airway evaluation in addition to measurements and volume analysis, for example.

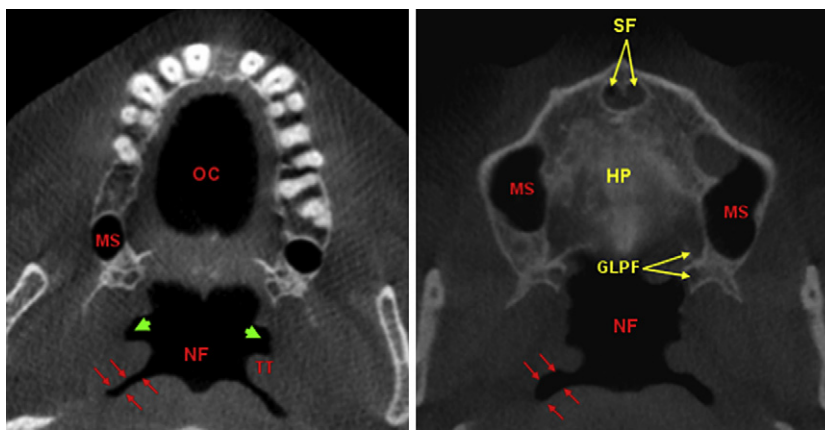

Fig. 15. (*Left*) Axial section at the level of the roots of the maxillary teeth. (*Right*) Axial section slightly superior to the other one, at the level of the floor of the maxillary sinus. GLPF, greater and lesser palatine foramina; HP, hard palate; MS, maxillary sinus; OC, oral cavity; SF, superior foramina, the starting point of the nasopalatine canal. The green arrows show the pharyngeal opening of the Eustachian tube, which helps in equalizing the pressure between the two sides of the eardrum. The red arrows mark fossa Rosenmüller. The torus tubarius (TT), a soft tissue process on either side of the nasopharynx separating the Eustachian tube, forms the fossa Rosenmüller.

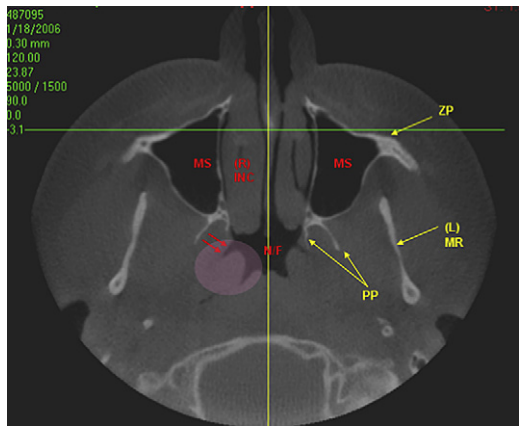

Fig. 16. Axial section at the level of the maxillary sinuses and mandibular rami demonstrates major structures of the maxillary sinus, nasal cavity, and nasopharynx at the axial plane. INC, inferior nasal concha; MR, mandibular ramus; MS, maxillary sinus; N/F, nasopharynx; PP, lateral and medial pterygoid plates; ZP, zygomatic process of the maxilla. The red arrows mark the Eustachian tube, and the round shaded region marks the general site of fossa Rosenmüller and torus tubarius.

(see Figs. 16 and 17). The nasal structures and the paranasal sinus are best visualized in coronal images (discussed elsewhere in this article).

Axial cuts toward the superior third of the maxillary sinuses show additional important anatomic structures (see Figs. 17 and 18). The dense

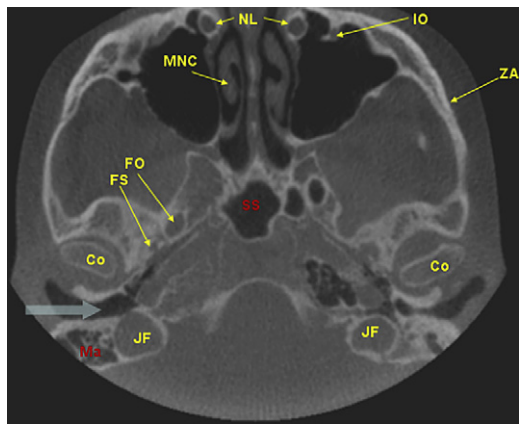

Fig. 17. Axial section at the level of the maxillary sinuses (superior third) demonstrates major structures of the maxillary sinuses, nasal cavity, and skull base at the axial plane. Co, mandibular condyle; FO, foramen ovale; FS, foramen spinosum; IO; infraorbital canal; JF, jugular foramen (or jugular fossa); Ma: mastoid air-cells; MNC, middle nasal concha; NL, nasolacrimal duct; SS, sphenoid sinus; ZA, zygomatic arch. The blue arrow indicates the external auditory canal.

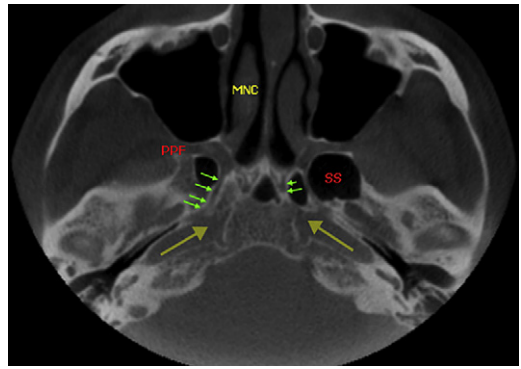

Fig. 18. Axial section at the level of the maxillary sinuses (superior third same as in Fig. 17, slightly higher) demonstrates additional anatomic details about the skull base. MNC, middle nasal concha; PPF, pterygopalatine fossa; SS, sphenoid sinus. The green arrows mark the walls of a thin channel known as the "Vidian canal" or pterygoid canal. The yellow arrows mark the course of the carotid canals, which appear to be converging toward the base of the sphenoid bone. The reader is reminded that the pterygopalatine fossa is a region of importance in the skull base. It is the passageway from the middle cranial fossa to the orbit, face, sinuses, and vice versa. Disease processes may be transferred from the middle cranial fossa to other sites (mentioned previously) through the pterygopalatine fossa. Similarly, disease originating extracranially may be transferred to the endocranium through the PPF.

arched-shaped structures seen on the lateral aspect of the face are the zygomatic arches. The anterior junction with the maxilla represents the zygomatomaxillary junction or suture in the anterior corner of the midface bilaterally.

The nasal septum is identified along the midline of the nasal cavity and is not always fully ossified. The middle nasal conchae are two of the osseous processes (six in total) that separate the nasal cavities in smaller chambers, the meati or turbinates. The two well-defined and well-corticated soft tissue content structures in the anterolateral wall of the nasal cavity bilaterally are the nasolacrimal ducts. The nasolacrimal ducts drain tears from the orbits to the inferior nasal turbinates.

Several important anatomic structures are identified posterior to the midface, in the skull base (see Figs. 17–19). These are the mandibular condyles, external auditory canals, and mastoid processes (partially visualized) bilaterally and the sphenoid sinus almost in the center of the axial image. Anteromedial to the mandibular condyles lay two important foramina: the foramen ovale (larger one) and the foramen spinosum (smaller one). The former hosts the third division of the trigeminal nerve (V3) and the mandibular nerve, and the latter hosts the middle meningeal artery.

At the same level, simply by slightly changing the reformatting angle to make our sections more parallel to the skull base, additional important anatomic structures appear. One of the most important anatomic regions

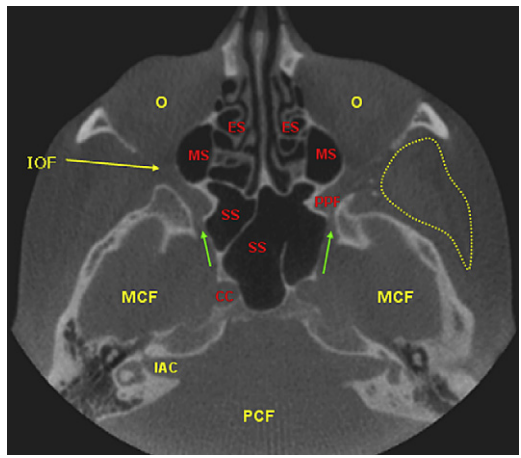

Fig. 19. Axial image of the head at level of the orbits (inferior third). The section depicts the roof of the maxillary sinuses bilaterally (MS) and the ethmoid sinuses (ES) just medial to the maxillary sinuses. Please note the fine and delicate air cells that form the ethmoid sinuses; this fine and complicated architecture has given the name of ethmoid labyrinth to the ethmoid air cells. The circular depressions toward the posterolateral walls of the sphenoid sinuses (SS), which can be seen in its magnitude in this image, represent the continuation of the carotid canals (CC) as they are entering the cavernous sinus of the lateral border of the base of the sphenoid bone. Note the septations present in the sphenoid sinus seen in this image. The section clearly illustrates the relation between the pterygopalatine fossa (PPF), the inferior orbital fissure (IOF), and the temporal fossa (*yellow dotted area*). Finally, the green arrows mark the course of the right and left foramen rotundum. IAC, internal auditory canal; MCF, middle cranial fossa; PCF, posterior cranial fossa.

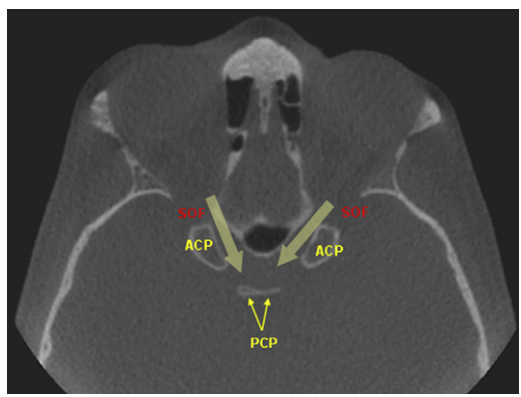

Fig. 20. Axial section of the head at the level of the orbits (superior half). The posterior opening of the orbits is divided to the superior orbital fissure (SOF) and the optic canal (*large yellow arrows*). The orientation of the optic canals is toward the sella turicica; this is the location of the optic chiasma. ACP, anterior clinoid processes; PCP, posterior clinoid processes.

of the skull base is the pterygopalatine fossa (PPF), which is identified in contact with the posterior wall of the right and left maxillary sinuses. The pterygopalatine fossa represents a major crossroad in the skull base. Two large osseous channels open in the PPF: the Vidian canal (or pterygoid canal), which hosts fibers of the petrosal nerves, and the foramen rotundum, which carries the maxillary nerve (V2). With the PPF as a passageway, the middle cranial fossa communicates with the orbits (through the inferior orbital fissure) and with the paranasal sinuses through the sphenopalatine foramen, the infratemporal fossa, and the nasal cavity. Through this crossroad, inflammation from the orbits, nasal cavity, sinuses, and oral cavity can be transferred into the middle cranial fossa and vice versa. The identification of the pterygopalatine fossa and assessment of the integrity of its margins are absolutely necessary if this structure is demonstrated in the CBCT scan [4,5].

Just posterior to the foramen ovale and medial to the mandibular condyle lays the carotid canal on either side of the skull base. The two canals converge toward the base of the sphenoid, where they pass close to the cavernous sinus before they ascend.

At the same level, almost in contact with the posterior border of the external auditory canals and medial to the mastoid air cells, the jugular foramina are visualized. Also known as jugular fossae (because of their large size), they are well defined, wide, corticated canals that serve as the passage points for the ninth, tenth, and eleventh cranial nerves and the jugular vein, among others. Variation in their shape and size in addition to asymmetry is not uncommon.

More cephalad sections (see Fig. 19) show the orbits, the ethmoid sinuses, and the sphenoid sinuses. The posterior opening of the orbits at that level is the inferior orbital fissure, which communicates with the pterygopalatine fossa as mentioned previously.

The ethmoid sinuses are made up of numerous, small, thin-walled air cells separated by the vomer bone (nasal septum), in the midline. Their complicated anatomy gave them the characterization of the ethmoid labyrinth.

The sphenoid sinus is located just posterior to the ethmoid sinuses. These are air cavities that are irregular in shape and size, located just below the base of the sphenoid bone. Anatomic variation and septations are often the rule rather than the exception.

As with all the air cavities that the author has defined and discussed so far, their healthy (normal) appearance is dark or black. When anything other than a dark appearance is noted, it may represent a pathologic entity in the region. The sinuses are evaluated and reviewed in more detail in the coronal images to visualize their relation to the nasal cavity and to each other better in addition to their draining.

The most superior axial sections reveal the upper half of the orbits, the temporal fossa, and parts of the middle and posterior cranial fossae. The concavities seen toward the posterolateral orbital walls are the temporal

fossae; they are anatomic depressions into the temporal bone and serve as the attachment point for the temporalis muscle (see Fig. 20).

At this level, the posterior opening of the orbits appears to be splitting into two distinct openings. The one medially, which appears to be converging toward the sella turcica and finally joining the contralateral one, is the optic canal. The optic canals host the optic nerves, which converge on the sella, forming the optic chiasma. The other opening is the superior orbital fissure. The linear structure along the midline demonstrating a transverse orientation, just posterior to the optic chiasma, is the posterior clinoid processes (see Fig. 20).

The author continues with the review of several anatomic structures in the coronal plane. It is strictly recommended so as to utilize fully the potential of multiplanar imaging to review and synthesize or reformat not only the anatomic structures of concern or the areas of interest in all three planes but to reformat images along custom-made planes or any plane that helps to differentiate the pathologic entity of interest and all the anatomic structures of interest.

Coronal sections are used for the evaluation of anatomic structures that have a posteroanterior orientation. The paranasal sinuses, structures of the nasal cavity, and certain structures in the skull base are going to be optimally imaged in this view. In this article, the author reviews the anatomic structures of interest starting from anterior to posterior (Figs. 21–26).

At the level of maxillary premolars, the coronal sections reveal the anterior aspect of the maxillary sinuses, a small portion of the frontal sinuses, and the orbits. A canal is identified toward the inferomedial wall of the orbit

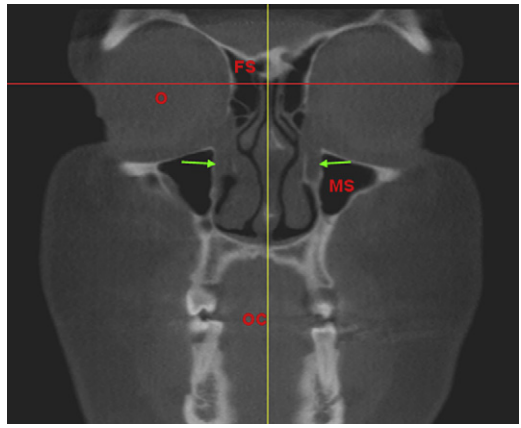

Fig. 21. Coronal section of the face approximately at the premolar level. The structures visualized at this level are the orbits (O), frontal sinuses (FS), oral cavity (OC), anterior walls of the right and left maxillary sinuses, and nasolacrimal ducts, marked by the green arrows.

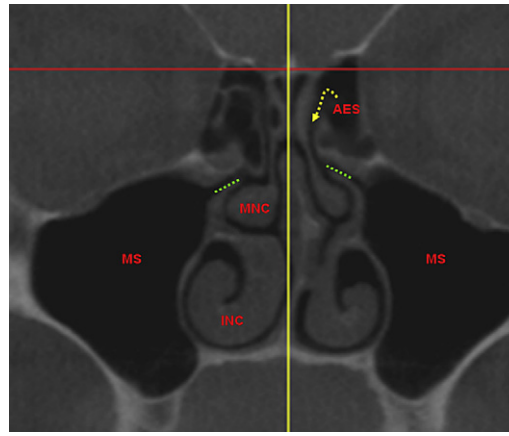

Fig. 22. Coronal section of the face approximately at the level of maxillary sinuses and nasal cavity (maxillary molar level). These images are optimal for the evaluation of the integrity of the floor and walls of the sinuses and nasal cavities. The draining site of the maxillary sinuses (osteomeatal complex) and ethmoid sinuses can be best evaluated in these sections (in this image, the draining channel is marked with a *green dotted line*). As you can see, the maxillary sinuses drain into the middle nasal turbinate (meatus). It is imperative that this structure is identified and assessed before possible sinus grafting procedures. The anterior ethmoid air cells (AES) drain close to those of the maxillary sinuses (*see curved yellow arrow*) in the middle nasal turbinate as well. INC, inferior nasal concha; MNC, middle nasal concha; MS, maxillary sinus.

(see Fig. 21); this is the nasolacrimal canal that originates on the floor of the orbit and drains into the inferior nasal turbinate.

The nasal anatomy and the anatomy of the maxillary sinuses can be reviewed best at the level of the maxillary molars. The nasal cavity is

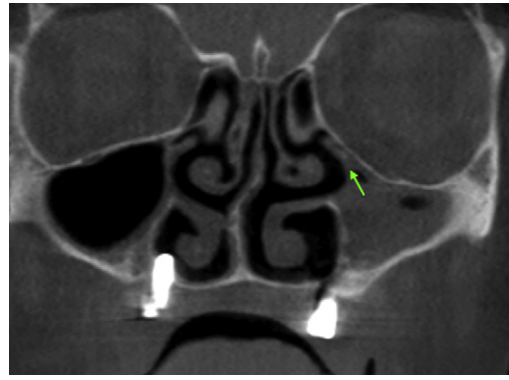

Fig. 23. Coronal section through the maxillary sinuses shows the presence of inflammatory tissue in the left maxillary sinus and thickening of the mucosal lining of the floor and walls of the right maxillary sinus. Note the blocked draining channel (ostium) marked by the green arrow.

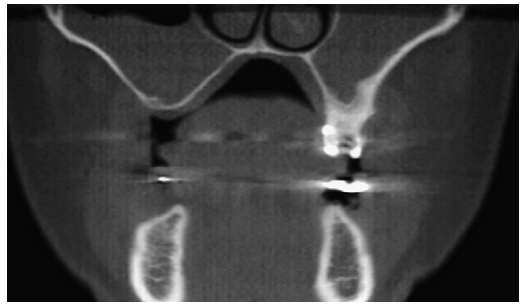

Fig. 24. Coronal section through the sinuses shows extensive inflammation (collection of soft tissue in density content in the sinus cavities) of the right and left maxillary sinuses. Also, note the severe pneumatization of the right sinus; it appears that the floor of the sinus and the crest of the alveolar ridge coincide.

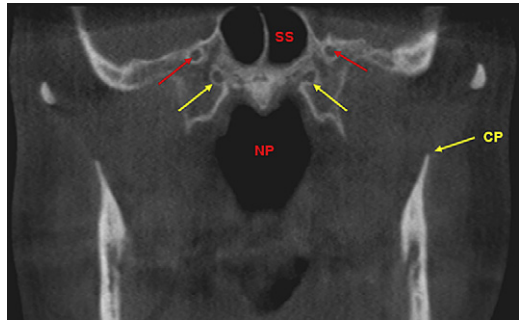

Fig. 25. Coronal section through the sphenoid sinus. CP, coronoid process of the mandible; NP, nasopharynx; SS, sphenoid sinus. The yellow arrows show the Vidian canal (pterygoid canal), and the red arrows show the foramen rotundum.

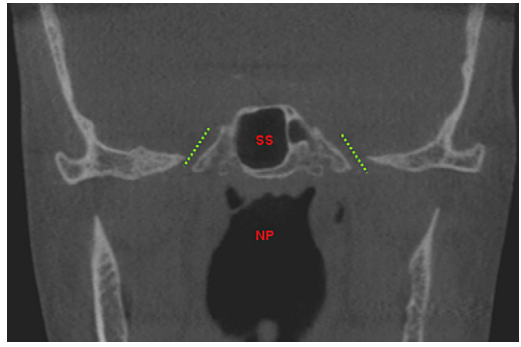

Fig. 26. Coronal section through the sphenoid sinus (just posterior to section in Fig. 25). SS, sphenoid sinus; NP, nasopharynx. The dotted green lines mark the course of the foramen ovale bilaterally.

separated into three distinct chambers (meati or turbinates) on either side of three osseous processes, the nasal conchae (inferior, middle, and superior). Only the inferior concha is an independent facial bone; the rest are parts of the ethmoid bone. The position of the nasal septum may contribute to the asymmetry between the right and left sides (see Fig. 22).

Coronal views toward the anterior third of the orbits will reveal the paper-thin plate of the ethmoid or lamina papyracea. At this level, the draining sites of the maxillary sinuses are likely to be visualized. In fact, they are narrow passageways toward the superomedial wall of the maxillary sinuses leading into the middle nasal turbinate; they are formed partially from the ethmoid bone (superior) and a thin pointy osseous process on the lateral wall of the nasal cavity known as the uncinate process. The site, as a whole, is known as the osteomeatal complex (see Fig. 22). Asymmetry between the right and left sides and variation from individual to individual are not uncommon. Identification of the draining sites and assessment of their integrity are important in patients who undergo sinus grafting procedures. Blockage of the draining site may prevent the aeration of the sinus cavity and result in accumulation of inflammatory products into the sinus (see Figs. 23 and 24). The fine detailed and delicate anatomy of the ethmoid sinuses may be grossly altered if prior sinus surgery has occurred.

Coronal sections through the sphenoid sinuses reveal the sphenoid sinus anatomy and variants. Last, most of the anatomic structures discussed previously in the axial plane can be identified in the coronal sections as well (see Figs. 25 and 26).

It is strongly recommended that to take advantage of the CBCT images in full, the diagnostician should be able to understand and apply the concept of multiplanar reformatting to the highest degree. It is in the dentist's hands to reveal the information related to each diagnostic task. In other words, our diagnostic efficiency is based on our sound knowledge of anatomy and on our skills to retrieve relevant diagnostic information.

References

[1] Kalpidis CD, Setayesh RM. Hemorrhaging associated with endosseous implant placement in the anterior mandible: a review of the literature. J Periodontol 2004;75(5):631–45.
[2] Tepper G, Hofschneider UB, Gahleitner A, et al. Computed tomographic diagnosis and localization of bone canals in the mandibular interforaminal region for prevention of bleeding complications during implant surgery. Int J Oral Maxillofac Implants 2001;16(1):68–72.
[3] Mupparapu M, Kim IH. Calcified carotid artery atheroma and stroke: a systematic review. J Am Dent Assoc 2007;138(4):483–92.
[4] Som PM, Curtin HD. Head and neck imaging. 3rd edition. St Louis (MO): Mosby; 1996.
[5] Harnsberger HR, Wiggins RH, Hudgins PA, et al. Diagnostic imaging head and neck. Manitoba (Canada): Canada Elsevier; 2005.